Subspace-based AOA estimation in mmWave NR system using power measurement with a single-port antenna array

Oleg Shmonin, Vitaliy Kuptsov, Sergey Trushkov, Kirill Ponur,
Georgij Serebryakov, Hao Wang, Jiankun Zhang, Anatoliy Krivelevich

Abstract

The paper is dedicated to the multipath angle of arrival (AOA) estimation problem in millimeter wave (mmWave) 5G NR communication system. The case of a phased antenna array with a single digital port is considered. In this scenario, the conventional highly accurate subspace-based algorithms cannot be applied because of hardware restrictions. We proposed a novel subspace-based algorithm called power-based root minimal polynomial method (PR-MPM) that uses the spatial power spectrum to get an approximation of the signal correlation matrix. The power spectrum is measured via the conventional beam sweeping procedure over a finite number of directions. The efficiency of the proposed method is studied using the high-realistic ray-tracing-based channel model applied in mmWave IEEE 802.11ay standard. Simulation results show that AOAs can be precisely estimated using only single-port power measurement.

Index Terms

Angle of arrival (AOA), millimeter wave communication, 5G NR, analog beamforming.

Oleg Shmonin, Vitaliy Kuptsov, Sergey Trushkov and Kirill Ponur are with WiSAVVY of Radio Lab NN Ltd., Nizhny Novgorod, Russia (e-mail: info@wisavvy.com).

Georgij Serebryakov is with Sitronics Labs, Moscow, Russia (e-mail: g.serebryakov@sitronics-labs.com).

Hao Wang and Jiankun Zhang are with Huawei Technologies Co., Ltd., Beijing 100095, China (e-mail: hunter.wanghao@huawei.com; zhangjiankun4@huawei.com).

Anatoliy Krivelevich is with MRC RTT lab, Huawei Technologies Co.,Ltd., Moscow, Russia (e-mail: krivelevich.anatoliy@huawei.com)

I. Introduction

The rapidly growing demands of data rate, latency and reliability have led 5G New Radio (NR) and Wi-Fi communication systems to millimeter-wave band [1], [2]. The millimeter wave (mmWave) allows one to occupy a huge frequency band delivering high channel capacity. Specifically, 3GPP NR FR2 supports bands of up to 400 MHz at carrier frequency 28 GHz. However, the other side of the coin is the excessively high path loss. In order to overcome this problem one uses massive antenna arrays and adaptive beamforming to provide a high gain. The majority of mmWave channel models assume that there are several strong propagation paths which are well separated and can be characterized with a certain angle of arrival (AOA) [3]–[5]. Thus, the information about AOAs is enough to provide effective beamforming. As a consequence, the problem of accurate AOA estimation is critical to mmWave beam management.

Here, the challenging issue is multipath AOA estimation in both line-of-sight (LOS) and non-line-of-sight (NLOS) channels. This problem cannot be effectively solved with the conventional beam scanning algorithm because of the resolution limitation and sidelobe power leakage.

At present, a lot of effective algorithms which allow one to estimate the quantity and AOAs of multiple radiation sources have been developed. The list includes, but not limited to such algorithms as MUSIC (Multiple Signal Classification), ESPRIT (Estimation of Signal Parameters via Rotational Invariant Techniques) and MPM (Minimal Polynomial Method) [6], [7]. All these algorithms consider signal as a vector in some linear space and exploit division of this space into signal and noise subspaces. MUSIC and ESPRIT distinguish these subspaces using eigenvalue decomposition of the signal correlation matrix; MPM uses the properties of the correlation matrix minimal polynomial for the same purposes. As a result, algorithms provide high-accurate AOA estimate and superresolution ability.

However, the conventional subspace-based algorithms cannot be applied in the current mmWave equipment. The reason is that these algorithms require the same number of digital ports as the number of antenna elements. Since vendors try to decrease the product cost, the beamforming procedure is typically performed in the analog domain using controlled phase shifters. It means that the number of digital ports is much less than the number of antenna elements. Moreover, the typical user equipment (UE) may contain only a single receiver.

One of a possible solution to this problem is beam-space algorithms that apply signal vector decomposition in some basis of the beamforming vectors [8]. The number of these vectors can

be less than the number of antenna elements if AOA is expected to be in some limited sector. In the case of single-port AOA estimation this signal decomposition can be performed in the time domain [9]–[12].

However, the presence of the phase hop effect between sequent signal measurements does not allow one to combine signals received by different beams at different times coherently. Moreover, there are other reasons including imperfect synchronization, uplink and downlink switching that make beam-space algorithms inapplicable.

In [13] authors proposed the power-based solution that applies an adaptive beamforming technique in order to minimize the received power. The result beamforming vector belongs to the noise subspace and provides a pattern with nulls at AOAs that could be estimated. It is similar to MUSIC algorithm, but only one noise subspace vector is used instead of the whole basis. As a result, the number of picks in the spatial spectrum is one less than the number of antenna elements. Thus, it is an open issue how to select actual AOAs.

The state-of-the-art AOA estimation techniques that are potentially applicable in real-world systems under the mentioned hardware restrictions (a single digital ports and the phase hop effect) employ the beamforming conception [14]–[16]. In other words, they use information about the main lobe of the beam pattern only and, consequently, they suffer from the beamwidth limitation and sidelobe power leakage. Some of them [16] are also affected by AOA quantization errors. All of that make an effective multipath AOA estimation difficult.

Therefore, we can conclude that to date there is no efficient power-measurment-based multiple-AOA-estimation technique that can be applied in analog-beamforming system. However, this kind of algorithm is necessary for intelligent beam management in the typical 5G mmWave user equipment. Specifically, it is essential in such challenging cases as blockage or Non-Discrete-Fourier-Trasform beamforming [17]–[20].

The main contribution of the paper is the following. We propose a novel subspace-based AOA estimation algorithm which can be applied under the mentioned hardware restrictions. In other words, it employes power measurements with analog beamforming. Moreover, to authors' awareness, it is the only AOA estimation algorithm that employes a subspace-based approach under uncoherent reception with beamforming and allows one to estimate both the number and AOAs of multiple dominating propagation paths.

The algorithm uses the conventional beam sweeping procedure to get a spatial power spectrum and to make the approximation of a signal correlation matrix unavailable for direct estimation.

The following steps are based on the Root MPM algorithm [7] that has been modified to consider the specific of the task. We have called the new AOA estimation technique as PR-MPM (Power-based Root Minimal Polynomial Method). The efficiency of the developed algorithm is compared with state-of-the-art power-based AOA estimation techniques that can also be applied under the mentioned hardware restrictions [14]–[16].

The rest of the paper is organized as follows. In Section II we provide the description of the signal model and the proposed PR-MPM algorithm. Factors influenced the accuracy are also discussed. Section III is dedicated to some special aspects of algorithm implementation in 5G NR. Simulation results are presented in Section IV and the conclusion of the paper is made in Section V.

Notations. The scalar values are noted as a; $\mathbf{a}$ is a vector and $\mathbf{A}$ is a matrix. The identity matrix is noted as $\mathbf{E}$. The angular brackets note the mathematical expectation and $\mathbf{a}^H$ is a Hermitian conjugate of vector $\mathbf{a}$.

II. General Algorithm Description

A. Signal Model

Let us consider a uniform linear antenna array (ULA) that consists of N elements with spacing d in the units of the wavelength. In the general case, we can assume the presence of J point-like correlated radiation sources which AOA should be estimated. In the case of the communication system, we can consider different propagation paths as virtual radiation sources.

Let us introduce spatial frequency $\psi = 2\pi d \sin\varphi$, where φ is AOA. The signal received by the antenna array can be represented as vector $\mathbf{h} = a_1\mathbf{s}(\psi_1) + \cdots + a_J\mathbf{s}(\psi_J) = \mathbf{Sa}$. Here a_j and ψ_j are the complex amplitude and the spatial frequency of the j-th source; $\mathbf{s}(\psi)$ is the steering vector of the flat wave arriving from angle φ; columns of matrix $\mathbf{S}$ are vectors $\mathbf{s}(\psi_j)$ and elements of vector $\mathbf{a}$ are a_j. The steering vector is defined as

$$\mathbf{s}(\psi) = \begin{bmatrix} 1 & e^{\psi} & \dots & e^{(N-1)\psi} \end{bmatrix}. \tag{1}$$

In the case of a digital antenna array, the received vector would be augmented with noise vector $\boldsymbol{\xi}$, i.e. $\mathbf{x} = \mathbf{h} + \boldsymbol{\xi}$. In this case the correlation matrix of the received signal would be presented as

$$\mathbf{M} = \langle \mathbf{x}\mathbf{x}^H \rangle = \mathbf{S}\mathbf{G}\mathbf{S}^H + \sigma^2 N^{-1}\mathbf{E}. \tag{2}$$

Here $\mathbf{G} = \langle \mathbf{a}\mathbf{a}^H \rangle$ is the correlation matrix of the radiation sources, $\mathbf{E}$ is the identical correlation matrix of the noise and σ^2 is the total noise power over all digital ports.

However, in the case of a single digital port, the real measured signal is $y = \mathbf{w}^H \mathbf{h} e^{i\eta} + \xi$, where ξ is a noise scalar, $\mathbf{w}$ is a beamforming vector and η is a random phase noise. Thus, under a single port restriction the correlation matrix (2) cannot be estimated directly.

B. Correlation Matrix Approximation

In order to apply a subspace-based algorithm it is necessary to build approximation $\mathbf{M}_a$ of the correlation matrix $\mathbf{M}$. However, what we can use is only the set of power values measured for different beam directions that is also known as the spatial power spectrum. The theory of the stochastic process states that the power spectrum of the signal is related to its correlation function through Fourier transformation. Thus, the same idea could be applied in the spatial domain to get the correlation vector of the antenna array. The precise correlation matrix $\mathbf{M}_a$ is Toeplitz matrix if radiation sources are independent. The first column of this matrix is the correlation vector. Thus, it is reasonable to apply the Toeplitz completion for correlation matrix approximation.

The Toeplitz completion is a well-known approach for matrix approximation. In AOA estimation field it has been used to overcome the signal sources correlation effect or for improving the correlation matrix of non-uniform arrays [6]. The proposed solution is a new application of this technique that targets to restore the correlation matrix basing on the measured spatial power spectrum.

Let us consider a spatial power spectrum $f(\psi)$ that can be obtained using beamforming vector $\mathbf{w} = \mathbf{s}(\psi)$ determined in (1).

$$f(\psi) = \langle |y(\psi)|^2 \rangle = \sum_{n=1}^{N} \sum_{m=1}^{N} \langle h_n h_m^* \rangle e^{i(m-n)\psi} + \sigma^2 \tag{3}$$

Noise power σ^2 can be brought under the sum signs using Kronecker delta δ_{nm}. Thus, we get that

$$f(\psi) = \sum_{n=1}^{N} \sum_{m=1}^{N} \mathbf{M}_{nm} e^{i(m-n)\psi} \tag{4}$$

Here $\mathbf{M}_{nm} = \langle h_n h_m^* \rangle + \sigma^2 N^{-1} \delta_{nm}$ is an element of the correlation matrix (2). Thus, the power spectrum obtained using an analog antenna array is related to the correlation matrix of an effective digital array.

One can see that $f(\psi)$ is a periodic function than can be expanded into a finite Fourier series, i.e.

$$f(\psi) = \sum_{q=1-N}^{N-1} D_q e^{iq\psi}, \tag{5}$$

$$D_q = \frac{1}{2\pi} \int_{-\pi}^{\pi} f(\psi) e^{-iq\psi} \mathrm{d}\psi. \tag{6}$$

Equation (6) can be approximated with a finite sum consisting of $2K$ terms

$$D_q \approx \frac{1}{2K} \sum_{k=-K}^{K-1} f\left(\pi \frac{k}{K}\right) e^{-i\pi \frac{kq}{K}}. \tag{7}$$

In case $K \to \infty$ approximation (7) equals to (6) for any index q. However, since the series consists of the finite number of non-zero terms with indexes $|q| < N$, the approximation becomes accurate for $K \geq N$. To prove it one could put (5) into (7), find the sum of the geometric progression and obtain the following:

$$\frac{1}{2K} \sum_{p=-N+1}^{N-1} D_p \frac{\sin(\pi(p-q))}{\sin\left(\frac{1}{2K}\pi(p-q)\right)} e^{i\pi \frac{q-p}{2K}} = D_q \tag{8}$$

From the other hand, we can see from (4) that $\mathbf{D}_q$ is the sum of q-th diagonal of the correlation matrix $\mathbf{M}$, i.e.

$$D_q = \sum_{n=1}^{N-q} \mathbf{M}_{n,n+q}, \;\; D_{-q} = D_q^*, \;\; q \geq 0. \tag{9}$$

Thus, using signal power measured at $2K$ beams we can obtain the correlation vector which elements $r_q = D_q(N - |q|)^{-1}$. In this case we can build an approximation of the correlation matrix using Toeplitz completion

$$\tilde{\mathbf{M}}_a = \begin{bmatrix} r_0 & r_1 & \dots & r_{N-1} \\ r_{-1} & r_0 & \dots & r_{N-2} \\ \vdots & \vdots & \ddots & \vdots \\ r_{1-N} & r_{2-N} & \dots & r_0 \end{bmatrix}. \tag{10}$$

Toeplitz completion is a well-known approach used in case of the coherent radiation sources [6]. This approximation may not be a positive definite matrix that leads to AOA estimation problems. To overcome this problem we propose to apply the regularization procedure

$$\mathbf{M}_a = \left[\mathrm{Tr}\left(\tilde{\mathbf{M}}_a\right)\right]^{-1} \tilde{\mathbf{M}}_a + \beta \mathbf{E}. \tag{11}$$

Here β is the regularization factor which set an additional virtual noise power.

Thus, we can build the correlation matrix approximation using the following steps.

Step 1. Measurements of the averaged power for at least $2K = 2N$ beams with beamforming vectors like (1) and spatial frequency spacing $\Delta\psi_{bf} = \pi K^{-1}$.

Step 2. Calculation of Fourier series (7) and approximation (10).

Step 3. Regularization procedure (11).

C. Approximation Errors

The accuracy of the correlation matrix approximation $\mathbf{M}_a$ depends on several factors. First of all, it is the quality of the power measurement (the number of samples employed for averaging). Another issue is the number of measured beams. If power is estimated precisely, we can accurately calculate the coefficients of the Fourier series provided condition $K \geq N$ is met. In the real system the discrete power spectrum estimate has errors. Thus, the more K is, the more accurate the result is due to error averaging. The last, but the most important point is the accuracy of Toeplitz completion (10). Let us consider the case when the power spectrum is estimated precisely and $K \geq N$. Also, let us assume that there are two radiation sources with equal power ν and correlation coefficient ρ. In this case, the elements of the correlation matrix could be represented as

$$\begin{aligned}\mathbf{M}_{n,n+q} =&\nu e^{-iq\psi_1} + \nu e^{-iq\psi_2} + \nu\rho e^{i(\psi_1-\psi_2)n-iq\psi_2} \\ &+ \nu\rho^* e^{i(\psi_2-\psi_1)n-iq\psi_1} + \sigma^2 N^{-1}\delta_q.\end{aligned} \tag{12}$$

Here ψ_1 and ψ_2 are spatial frequencies of the radiation sources and δ_q is the discrete Dirac delta function. Combining (9) and (12) one can get that

$$\begin{aligned}r_q =&\nu e^{-iq\psi_1} + \nu e^{-iq\psi_2} \\ &+ 2\nu|\rho|\frac{\sin\left(\frac{1}{2}(N-|q|)\Delta\psi\right)}{(N-|q|)\sin\left(\frac{1}{2}\Delta\psi\right)} e^{-i\psi_0 q} \times \cos\left(\frac{1}{2}(N-q+1)\Delta\psi + \chi\right) + \sigma^2 N^{-1}\delta_q.\end{aligned} \tag{13}$$

Here $\psi_0 = 0.5(\psi_1 + \psi_2)$ is a middle spatial frequency; $\Delta\psi = \psi_1 - \psi_2$ is the spatial frequency spacing between sources and $\chi = \arg\rho$ is a phase of the correlation coefficient.

Thus, one can see that the correlation matrix approximation before the regularization can be presented as

$$\tilde{\mathbf{M}}_a = \nu\mathbf{S}\mathbf{E}\mathbf{S}^H + \mathbf{B} + \sigma^2 N^{-1}\mathbf{E}. \tag{14}$$

Here elements of matrix $\mathbf{B}$ are set using the third term in (13).

Let us compare (2) and (14). First of all, we can see that correlation matrix $\mathbf{G}$ of radiation sources is replaced with identity matrix $\mathbf{E}$. Thus, one can consider them as independent. The second point is related to extra matrix $\mathbf{B}$. It is not positive definite. The power spectrum obtained for this matrix is symmetrical with respect to middle spatial frequency ψ_0 and it may have negative values. This extra matrix provides an inevitable approximation error that affects AOA estimation. If radiation sources are uncorrelated (i.e. the power of the aggregated signal is a sum of powers and $\rho = 0$), $\mathbf{B} = 0$, i.e. (2) and (14) are the same (approximation is accurate). If radiation sources are correlated, the wider spacing is, the more appropriate approximation (14) is.

D. Root Minimal Polynomial Method

The original Root MPM algorithm was proposed in [7]. It provides pretty well results and surpasses MUSIC in case of highly correlated signal sources, that was shown via natural experiments [21]. Moreover, it provides a quite flexible and robust tool for estimation of radiation sources number. It is especially important under correlation matrix approximation errors. It is why we have chosen Root MPM as the base of the developed algorithm. Other subspace-based algorithms (e.g. MUSIC or ESPRIT) and criteria (e.g. AIC or MDL) could also be employed [6]. However, it is an issue how they are affected with correlation matrix approximation and if they require some modifications.

MPM algorithm is based on Cayley-Hamilton theorem. It states that the correlation matrix (2) satisfies its own characteristic equation which can be reduced to the minimal polynomial via the removal of the repeated roots. The degree of this polynomial m is determined by the number of radiation sources (i.e. $m = J + 1$) and parameters of this polynomial can be used to separate noise and signal subspaces [7]. The main idea of the MPM algorithm is to approximate minimal polynomial of the correlation matrix (2) with some matrix polynomial of the correlation matrix approximation (11). For that we need to calculate metric I_m which has a sense of the square approximation error.

$$I_m = \min_{\gamma_1 \dots \gamma_m} \mathrm{Tr} \left[\prod_{k=1}^{m} (\mathbf{E} - \gamma_k \mathbf{M}_a)^2 \right] \tag{15}$$

Parameters γ_k have a sense of the estimate of the inverse eigenvalues of matrix $\mathbf{M}$. To find the extremum of the functional (15) one can use the numerical procedure given in [7] or analytical solution ($m \leq 4$) presented in [21].

To obtain an appropriate approximation of the minimal polynomial and estimate the number of sources, one needs to consistently consider hypotheses about the number of radiation sources $J = 0, \ldots, N-1$ and compare the corresponding metric I_{J+1} with some predefined threshold T until $I_{J+1} < T$. In this case, J is the estimate of the number of sources. The choice of the threshold value will be discussed below.

Obtained parameters γ_k can be used to construct the noise subspace projector

$$\mathbf{P} = \left[\prod_{k=1}^{J} (\mathbf{E} - \gamma_k \mathbf{M}_a)\right] \left[\prod_{k=1}^{J} \left(1 - \frac{\gamma_k}{\gamma_{J+1}}\right)\right]^{-1}. \tag{16}$$

Here we assume that $\gamma_{J+1} = \max_k(\gamma_k)$.

The property of the steering vector (1) is that it has a zero projection on the noise subspace if it is related to a certain radiation source, i.e.

$$\|\mathbf{P}\mathbf{s}(\psi_j)\|^2 = 0. \tag{17}$$

Thus, we can introduce new variable $z = \exp(i\psi)$ and write (17) as a polynomial

$$\mu(z) = \sum_{n=1-N}^{N-1} a_n z^n = 0. \tag{18}$$

Coefficients of this polynomial are given with

$$a_n = \sum_{k=1}^{N-n} \left[\mathbf{P}^2\right]_{k,k+n}; \quad a_{-n} = a_n^*; \quad n \geq 0. \tag{19}$$

There are some important properties of this polynomial. The first one is that if z is a root, then $1/z^*$ is also a root. The second is related to signal roots, i.e. roots corresponding to the radiation sources. If the noise subspace projector is estimated precisely, the signal roots have the second order and lay on the unit circle on the complex plane. As we cannot get the precise projector because of approximation and power measurement errors, the last property is not met in the real system. There are two similar signal roots for each radiation source. In the conventional Root MPM algorithm it is assumed that signal roots lay near the unit circle, but their absolute value is not equal to one in the real system. In our case, because of Toeplitz completion (10) signal roots related to a certain source may still lay on the unit circle in the real system. Thus, the convention approach [7] (to select signal roots with absolute value less than one) is not appropriate here and we have to modify it.

First of all, we need to sort roots in the descending order of their distance to the unit circle. Next, we consider the sorted list step by step and make pairs grouping roots with

similar phases. Let us consider root z_q, in this case the index of the other root in the pair is $m = \arg\min_m \left|1/z_q^* - z_m\right|$. When the pair is made, both roots are precluded from the sorted list and we move to the next pair. The last J obtained pairs correspond to radiation sources. The estimate of AOA for each pair is

$$\varphi = \arcsin\left[\frac{\arg z_q + \arg z_m}{4\pi d}\right]. \tag{20}$$

E. Threshold choice

Threshold T selection is an important issue. In the original Root MPM is recommended to use the expected value of metric I_1 under condition $J = 0$. In our case, one can calculate (see Appendix) it approximately as

$$T_1 = \frac{2N^2 H_{N-1}}{(2KL+1)(1+\beta N)^2 + 2NH_{N-1}}. \tag{21}$$

Here L is the number of independent samples used for power estimation at each beam and H_{N-1} is a harmonic number [22]

$$H_{N-1} = \sum_{n=1}^{N-1} \frac{1}{n} \approx \ln(N-1) + \frac{1}{2}N^{-1} + 0.5772. \tag{22}$$

The presented threshold T_1 is appropriate to check hypotheses $J = 0$ and $J = 1$. However, in case $J \geq 2$ it can lead to false alarms because of correlation matrix approximation error such as extra matrix $\mathbf{B}$ in (14). In this case, we propose an empirical threshold $T_2 = N - J_{max} - 2$, where J_{max} is the maximal expected number of radiation sources.

III. Algorithm Application Under 5G NR Beam Management Protocol

The proposed PR-MPM algorithm can be applied in the 5G NR system at UE side using the conventional beam training procedure. Let us assume that the base station (BS) periodically sounds Q beams using the synchronization signal burst set (SS-burst) as the reference signals (see Fig. 1). The current standard supports Q values up to 64 [2]. UE consistently receives signals for each BS's beam using $2K$ different UE's beams. Thus, the total number of sounded beam pairs is $2QK$.

Let $\mathbf{H}_s$ be the channel matrix at subcarrier s and $\mathbf{u}_q$ is q-th beamforming vector of BS. In this case, the received signal is $y_{s,q,k} = \mathbf{w}_k^H \mathbf{H}_s \mathbf{u}_q + \xi_{s,q,k}$, where $\mathbf{w}_k = \mathbf{s}(\pi k K^{-1})$ and k is in the range from $-K$ to $(K-1)$.

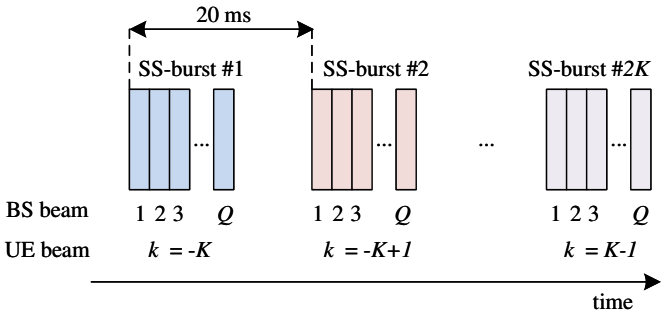

Fig. 1. Timeline of the 5G NR beam training procedure

For each UE's beam the received power can be averaged over both BS's beams and subcarriers, i.e.

$$f(\pi k K^{-1}) = \frac{1}{QL} \sum_{s=1}^{L} \sum_{q=1}^{Q} |y_{s,q,k}|^2. \tag{23}$$

Next, the algorithm described in section II is applied. The algorithm flowchart is presented in Fig. 2. Here we would like to note the following thing. In the general case, the signals propagating along different paths are expected to be highly correlated. However, there are two factors that decline signal correlation in the power spectrum (23) and improve correlation matrix approximation quality.

First of all, it is a spatial selection performed by BS's beams. If a certain BS's beam radiates the most power toward a certain propagation path and does not do it toward others, the power received by UE from these paths is combined incoherently in (23), i.e. $\rho \approx 0$. The narrower BS's beam is, the better result is. A similar effect could be achieved if BS used the random beamforming vectors. The second factor is the different time of arrival (TOA) of different propagation paths. In this case, the signal propagating along these paths has unique complex amplitudes at each subcarrier. It also leads to correlation factor reduction. Thus, despite the common signal source for different propagation paths, the way how power spectrum (23) is estimated allows one to significantly decrease the correlation between different propagation paths. Therefore, it leads to appropriate quality of correlation matrix approximation (11) and AOA estimate accuracy.

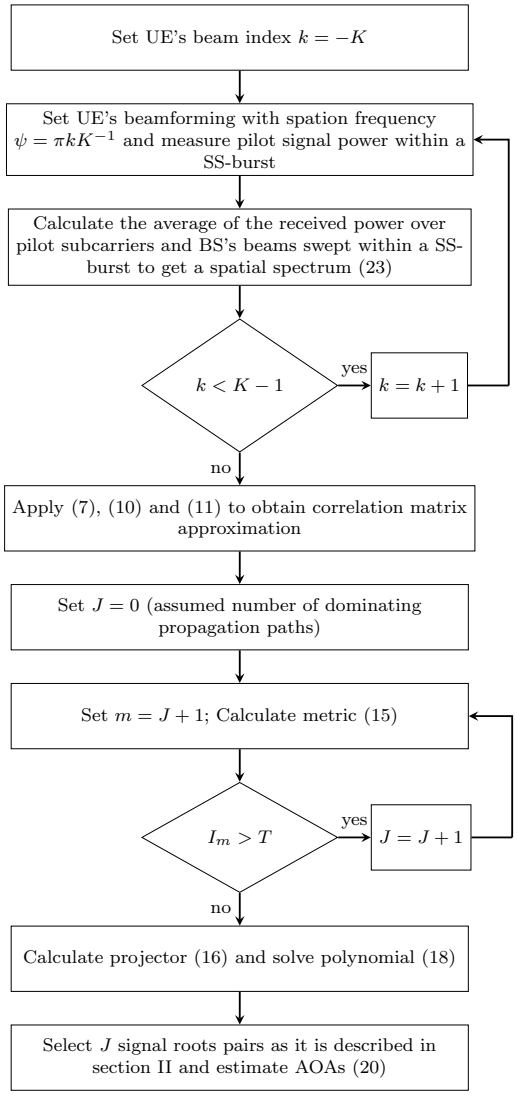

Fig. 2. The algorithm flowchart.

IV. Simulation Results

The proposed PR-MPM algorithm was verified using the high-realistic ray-tracing-based channel model applied in mmWave IEEE 802.11ay standard [5]. As the base scenario the Hotel Lobby was considered. It represents a typical indoor scenario with a large hall (the length is 20 m, the width is 15 m and the height is 6 m) and pronounced multipath propagation. The BS was located near a wall (with a gap 1 m) at a height of 5.5 m. The UE was located at different points of the hall at a height of 1.5 m in accordance with the model.

Two scenarios were considered: LOS channel and NLOS channel. To provide NLOS channel

additional wall blocking LOS ray was added in the middle of the hall.

BS had a rectangular antenna array with 8 rows, 16 columns and element spacing equal to the half of the wavelength. UE had a ULA with 8 elements and half-wavelength spacing. The antenna element pattern was modeled as described in 3GPP TR 38.901 [23]. The polarization was vertical.

The NR system working at carrier frequency 28 GHz was modeled. The sample rate was set at 61.44 MHz. The subcarrier spacing was 120 kHz. FFT size was 512. SS-burst was considered as a reference signal. Thus, only 127 central subcarriers were used for power measurement [2]. The total transmitted power was 10 dBm in the LOS scenario and 23 dBm in the NLOS scenario. The algorithm was implemented as it is described in Section III. The regularization factor β was set to 0.02.

As the information about two dominating paths (the strongest main path and the backup path) is typically enough to maintain a stable connection, the maximal number of detected sources was set to 2. The results are presented for a certain LOS case in Fig. 3 and for a certain NLOS case in Fig. 4. The black arrow is showing BS position and direction. The grin arrow is showing UE position and direction. The beam scanning result in the polar coordinate system is plotted with a blue line. The red arrows are depicting AOAs found by the developed algorithm (the main and backup paths). The corresponding propagation paths are shown with the solid magenta lines. In the LOS scenario it is a LOS ray and a single bounce reflected ray. In the NLOS scenario it is a single and double bounce reflected rays. Other weaker paths are represented with dash grey lines.

It can be seen that the proposed algorithm allowed one to successfully detect and estimate AOAs of the most important propagation paths using only single-port power measurement.

Simulation results for some other UE positions (x, y) are presented in Table I. Angle α describes UE rotation (orientation) from the x-axis (contraclockwise). The estimated AOAs values φ were compared with the effective AOAs of the corresponding propagation paths which were calculated as $\varphi_{eff} = \arcsin(\sin\varphi_g \cos\theta_g)$ based on geometrical azimuth φ_g and elevation angle θ_g so that it provided the same spatial frequency $\psi = 2\pi d \sin\varphi_{eff}$. The AOA estimation error was evaluated. All angles are given in degree units.

One can see that in the majority of cases the developed algorithm found the main and backup paths with a quite high accuracy. However, if the main path was amplified by the antenna element pattern and significantly surpassed all backup paths (e.g. cases #7-12 in Table I), no backup path

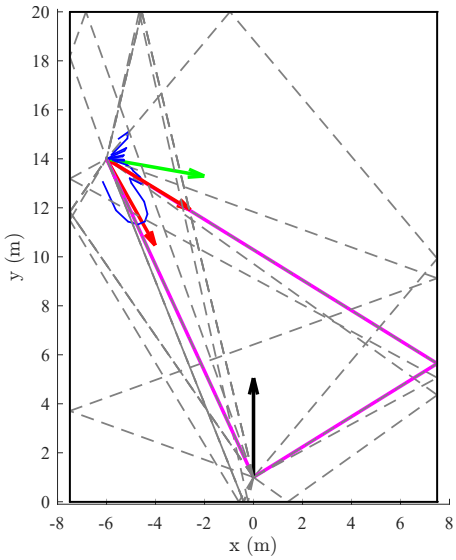

Fig. 3. AOAs result in LOS channel

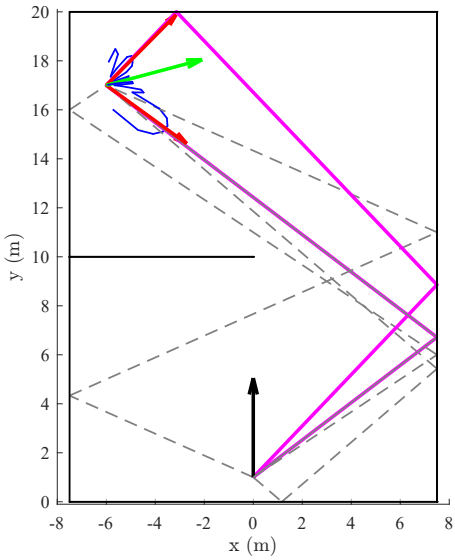

Fig. 4. AOAs result in NLOS channel

was found because of regularization (11). In these cases, $\mathrm{Tr}\,\tilde{\mathbf{M}}_a$ was determined by the strongest eigenvalue and all other signal subspace eigenvalues were suppressed below β value.

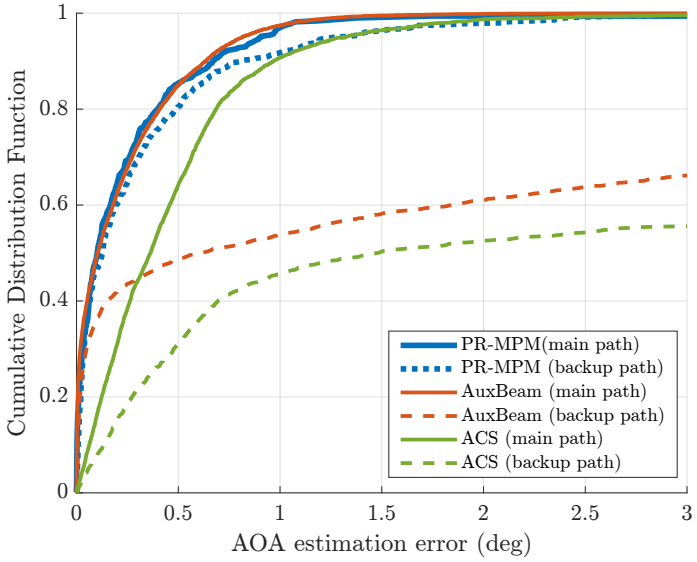

Fig. 5. AOAs error is NLOS channel

Additionally, we conducted Monte-Carlo Simulations for NLOS case as the most challenging one. The UE position (x, y) was randomly set within the LOS-ray shadow area. The orientation α was also set randomly from -180 to 180 deg. The UE's antenna system was augmented with

TABLE I

SIMULATION RESULTS

#	Parameters			The main path		The backup path	
	State	(x, y)	α	φ	ε	φ	ε
1	LOS	(-6, 11)	0	-24.89	0.18	-51.68	2.53
2	LOS	(-6, 14)	-10	-21.29	0.18	-50.65	1.64
3	LOS	(-6, 17)	-10	-26.85	0.12	-54.95	2.03
4	LOS	(-6, 6)	-80	-2.22	0.17	32.63	2.43
5	LOS	(-2, 11)	0	-29.29	0.51	-62.14	3.77
6	LOS	(-2, 14)	-30	-7.28	0.001	-46.98	1.28
7	LOS	(-2, 17)	-80	-2.72	0.07		
8	LOS	(-2, 6)	-80	8.90	0.55		
9	LOS	(5, 11)	-80	-32.92	1.20		
10	LOS	(5, 14)	-80	-28.72	0.98		
11	LOS	(5, 17)	-80	-25.95	0.60		
12	LOS	(0, 11)	-80	-8.97	0.31		
13	NLOS	(-6, 14)	15	-45.59	0.39	35.10	0.43
14	NLOS	(-6, 17)	15	-50.93	0.54	30.30	0.74
15	NLOS	(-2, 11)	15	-32.08	0.02	43.28	0.05
16	NLOS	(-2, 14)	35	-68.19	0.03	20.49	0.10
17	NLOS	(-2, 17)	25	-65.01	0.26	26.99	0.02

additional ULA that is the same as the initial one but rotated at 180 deg. Thus, the first ULA was in charge of AOAs from -90 to 90 deg and the second one was in charge of angle range from 90 to 270 deg. The developed method was applied independently for both ULAs. Estimated AOAs were combined. Two estimated AOAs providing the maximal value of the measured power spectrum were considered the main and backup paths. The estimated AOAs were compared with effective azimuths of the corresponding propagation paths. The obtained cumulative distribution function of the AOA estimation error is presented in Fig. 5.

The backup path was always found. The mean square error is 0.48 deg for the main path and 0.87 deg for the backup path. The median error value is about 0.12 deg for both paths.

The developed algorithm was compared with the state-of-the-art power-based AOA estimation methods that also use a single digital port. They were the Auxiliary Beam technique (AuxBeam) [14], [15] and Adaptive Compressed Sensing (ACS) [16].

The AuxBeam is a monopulse-like method that employs the sum-to-diff power ratio of neighbour orthogonal beams as a metric to estimate the AOA. It tested $(Q \times N)$ BS-UE's beam pairs (UE's beams are orthogonal) and selected the best one. For the selected BS's beam the best

”neighbour” of the UE’s beam was taken to calculate the metric and estimate AOA. To increase accuracy it may have required performing some additional power measurements in accordance with [15]. Thus, it is how the main path AOA was estimated. To evaluate the backup path one needed to select another BS-UE’s beam pairs. However, pairs that exceeded the sidelobe level of the main path were precluded.

The Adaptive Compressed Sensing [16] has sense of the ”binary” search. At each iteration, it tested four UE’s sectors (beams) for every BS’s beams. Among these four sectors it selected the two best and split them half. The algorithm started with four beams with a width about 90 deg. At each following iteration, the beamwidth should have been decreased by half. The beam width was controlled by switching on/off the antenna elements. At the first iteration, only two elements were used at each ULA. At the next one, it used four antenna elements, etc. However, at late iterations it could change beam (sector) direction only because all elements had been already switched on. For the considered antenna configuration the number of iterations was 8.

The results for AuxBeam and ACS techniques are also presented in Fig. 5. One can see that for the main path the efficiency of AuxBeam and PR-MPM algorithms are the same. ACS has quantization error, unlike the other algorithms, that leads to some performance degradation. As for the backup path, the best solution is provided by the PR-MPM algorithm, because it was specially designed for the multi-path case using substantially different signal properties and representation. This algorithm is not affected by the sidelobe power leakage problem because it does not use the power spectrum as a search function. Thus, the PR-MPM algorithm is more flexible when it comes to the second path detection. The worst result is provided by the ACS sensing algorithm which is significantly affected by the sidelobe leakage problem. In 57% of cases, it found the main path as the backup (they have been excluded from CDF statistic). Furthermore, some paths that are distinguishable with narrow beams might subtract each other at early stages with wide beams. Thus, wrong sector selection at early iterations (where the antenna gain is low) leads to totally wrong results at the following iterations.

As for the AuxBeam, it did not find the backup path in 1% of cases. The mean square (median) error of AuxBeam is 0.31 (0.12) deg for the main path and 4.26 (0.61) deg for the backup path. The mean square (median) error of ACS is 0.68 (0.36) deg for the main path and 5.83 (1.47) deg for the backup path.

V. Conclusion

We proposed a novel subspace-based AOA estimation algorithm called PR-MPM which can be applied in conjunction with a phased antenna array of mmWave NR UE under a single digital port restriction and phase hop effect. The algorithm uses a spatial power spectrum obtained via conventional beam scanning to make a correlation matrix approximation. The obtained approximation is processed using the adapted Root MPM method to estimate the number and AOAs of different propagation paths. The simulation results obtained for high-realistic ray-tracing-based channel model verifies the efficiency of the proposed algorithm. Note that other subspace-based algorithms (e.g. MUSIC or ESPRIT) could also be applied to the approximated correlation matrix, but it is an issue for further investigation.

Appendix

Let us obtain threshold (21) following the concept described in [24]. First of all, let us note that $\mathrm{Tr}\,\tilde{\mathbf{M}}_a = D_0$. Let us also set that there is no radiation source (i.e. $J = 0$). In this case, one can get from (15) that

$$I_1 = N - \frac{\mathrm{Tr}^2(\tilde{\mathbf{M}}_a + \beta D_0 \mathbf{E})}{\mathrm{Tr}\Big(\tilde{\mathbf{M}}_a + \beta D_0 \mathbf{E}\Big)^2}. \tag{24}$$

We expect that denominator varies little [24], so the numerator and denominator could be averaged separately to get an approximation of $\langle I_1 \rangle$. As for the numerator,

$$\langle \mathrm{Tr}^2(\tilde{\mathbf{M}}_a + \beta D_0 \mathbf{E}) \rangle = \langle D_0^2 \rangle (1 + \beta N)^2. \tag{25}$$

If $\xi_{k,j}$ is white Gaussian noise received with k-th beam at l-th sample, we can write based on (7) that

$$D_q = \frac{1}{2KL} \sum_{k=-K}^{K-1} \sum_{l=1}^{L} \xi_{k,l} \xi_{k,l}^* \exp\left(-i\pi \frac{kq}{K}\right), \tag{26}$$

where L is the number of independent samples used for power estimation.

Let us take into consideration the properties of the Gaussian complex random values and sample independence

$$\langle \xi_{k,l} \xi_{k,l}^* \xi_{h,g} \xi_{h,g}^* \rangle = \sigma^4 (1 + \delta_{kh} \delta_{lg}), \tag{27}$$

where δ_{kh} is Kronecker delta. In this case we can get that

$$\langle D_0^2 \rangle = \sigma^4 (1 + 0.5 K^{-1} L^{-1}). \tag{28}$$

As for the denominator of (24)

$$\langle \mathrm{Tr}\Big(\tilde{\mathbf{M}}_a + \beta D_0 \mathbf{E}\Big)^2 \rangle = \langle \mathrm{Tr}\, \tilde{\mathbf{M}}_a^2 \rangle + (2\beta + \beta^2 N)\langle D_0^2 \rangle. \tag{29}$$

Here the second term can be evaluated using (28). The first term is obtained basing on (10) as

$$\langle \mathrm{Tr}\, \tilde{\mathbf{M}}_a^2 \rangle = \sum_{s=1}^{N} \sum_{m=1}^{N} \frac{1}{(N - |m-s|)^2} \langle D_{m-s} D_{m-s}^* \rangle. \tag{30}$$

Using (26) and (27) in (30) we can obtain after some math transformations that

$$\langle \mathrm{Tr}\, \tilde{\mathbf{M}}_a^2 \rangle = \sigma^4 N^{-1} + 0.5 K^{-1} L^{-1} (H_N + H_{N-1}), \tag{31}$$

where H_N is the harmonic number (22).

Next, one can get (21) recasting (24) using obtained equations. Verification via numerical simulation showed a good match between the derived approximation of $\langle I_1 \rangle$ and averaged over experiments values.

ACKNOWLEDGMENT

We thank sincerely the authors of the original MPM algorithm prof. Victor T. Ermolaev and prof. Alexander G. Flaksman for the invaluable theoretical base and experience that they have shared with us during our education and research collaboration.

REFERENCES

[1] P. Zhou, K. Cheng, X. Han, *et al.*, "IEEE 802.11ay-based mmWave WLANs: Design challenges and solutions," *IEEE Communications Surveys & Tutorials*, vol. 20, no. 3, pp. 1654–1681, 2018. DOI: 10.1109/comst.2018.2816920.

[2] E. Dahlman, S. Parkvall, and J. Skold, *5G NR : The Next Generation Wireless Access Technology*. London: Academic Press, 2018.

[3] T. S. Rappaport, G. R. MacCartney, M. K. Samimi, and S. Sun, "Wideband Millimeter-Wave Propagation Measurements and Channel Models for Future Wireless Communication System Design," *IEEE Transactions on Communications*, vol. 63, no. 9, pp. 3029–3056, 2015. DOI: 10.1109/tcomm.2015.2434384.

[4] R. J. Weiler, M. Peter, W. Keusgen, *et al.*, "Quasi-deterministic millimeter-wave channel models in MiWEBA," *EURASIP Journal on Wireless Communications and Networking*, vol. 2016, no. 1, 2016. DOI: 10.1186/s13638-016-0568-6.

[5] A. Maltsev, "Channel Models for IEEE 802.11ay," *IEEE doc. 802.11-15/1150r9*, Mar. 2017.

[6] E. Tuncer and B. Friedlander, *Classical and modern direction-of-arrival estimation*. 2009.

[7] V. T. Ermolayev, A. G. Flaksman, A. V. Elokhin, and O. A. Shmonin, "Angular Superresolution of the Antenna-Array Signals Using the Root Method of Minimum Polynomial of the Correlation Matrix," *Radiophysics and Quantum Electronics*, vol. 61, no. 3, pp. 232–241, 2018. DOI: 10.1007/s11141-018-9884-5.

[8] M. Zoltowski, G. Kautz, and S. Silverstein, "Beamspace Root-MUSIC," *IEEE Transactions on Signal Processing*, vol. 41, no. 1, p. 344, 1993. DOI: 10.1109/tsp.1993.193151.

[9] C. Plapous, J. Cheng, E. Taillefer, A. Hirata, and T. Ohira, "Reactance Domain MUSIC Algorithm for Electronically Steerable Parasitic Array Radiator," *IEEE Transactions on Antennas and Propagation*, vol. 52, no. 12, pp. 3257–3264, 2004. DOI: 10.1109/tap.2004.836433.

[10] E. Taillefer, A. Hirata, and T. Ohira, "Reactance-domain ESPRIT algorithm for a hexagonally shaped seven-element ESPAR antenna," *IEEE Transactions on Antennas and Propagation*, vol. 53, no. 11, pp. 3486–3495, 2005. DOI: 10.1109/tap.2005.858854.

[11] E. Taillefer, W. Nomura, J. Cheng, M. Taromaru, Y. Watanabe, and T. Ohira, "Enhanced Reactance-Domain ESPRIT Algorithm Employing Multiple Beams and Translational-Invariance Soft Selection for Direction-of-Arrival Estimation in the Full Azimuth," *IEEE Transactions on Antennas and Propagation*, vol. 56, no. 8, pp. 2514–2526, 2008. DOI: 10.1109/tap.2008.927501.

[12] C. Sun and N. C. Karmakar, "Direction of Arrival Estimation with a Novel Single-Port Smart Antenna," *EURASIP Journal on Advances in Signal Processing*, vol. 2004, no. 9, 2004. DOI: 10.1155/s111086570431108x.

[13] S. Farzaneh and A. R. Sebak, "Single-port direction of arrival estimation using adaptive null-forming," in *2009 IEEE Antennas and Propagation Society International Symposium*, IEEE, 2009. DOI: 10.1109/aps.2009.5171463.

[14] D. Zhu, J. Choi, and R. W. Heath, "Auxiliary beam pair enabled aod and aoa estimation in mmwave fd-mimo systems," in *2016 IEEE Global Communications Conference (GLOBECOM)*, Dec. 2016, pp. 1–6. DOI: 10.1109/GLOCOM.2016.7841616.

[15] S. Kim, H. Han, N. Kim, and H. Park, "Robust beam tracking algorithm for mmwave mimo systems in mobile environments," in *2019 IEEE 90th Vehicular Technology Conference (VTC2019-Fall)*, Sep. 2019, pp. 1–5. DOI: 10.1109/VTCFall.2019.8891561.

[16] A. Alkhateeb, O. El Ayach, G. Leus, and R. W. Heath, "Channel estimation and hybrid precoding for millimeter wave cellular systems," *IEEE J. Sel. Topics Signal Process.*, vol. 8, no. 5, pp. 831–846, Oct. 2014. DOI: 10.1109/JSTSP.2014.2334278.

[17] M. Park and H. K. Pan, "A spatial diversity technique for ieee 802.11ad wlan in 60 ghz band," *IEEE Commun. Lett.*, vol. 16, no. 8, 1260–1262, Aug. 2012. DOI: 10.1109/LCOMM.2012.060112.120793.

[18] S. Kwon and J. Widmer, "Multi-beam power allocation for mmwave communications under random blockage," in *2018 IEEE 87th Vehicular Technology Conference (VTC Spring)*, 2018, pp. 1–5. DOI: 10.1109/VTCSpring.2018.8417624.

[19] Z. Xiao, "Suboptimal spatial diversity scheme for 60 ghz millimeter-wave wlan," *IEEE Communications Letters*, vol. 17, no. 9, pp. 1790–1793, 2013. DOI: 10.1109/LCOMM.2013.071813.131181.

[20] B. Gao, Z. Xiao, C. Zhang, L. Su, D. Jin, and L. Zeng, "Double-link beam tracking against human blockage and device mobility for 60-ghz wlan," in *2014 IEEE Wireless Communications and Networking Conference (WCNC)*, 2014, pp. 323–328. DOI: 10.1109/WCNC.2014.6951988.

[21] V. T. Ermolayev, A. G. Flaksman, A. V. Elokhin, and O. Shmonin, "An Experimental Study of the Angular Superresolution of Two Correlated Signals Using the Minimum-Polynomial Method," *Radiophysics and Quantum Electronics*, vol. 61, no. 11, pp. 841–852, 2019. DOI: 10.1007/s11141-019-09941-6.

[22] R. Graham, D. Knuth, and O. Patashnik, "Harmonic numbers," in *Concrete Mathematics: A Foundation for Computer Science*. New York, USA: Addison Wesley, Feb. 1994, pp. 272–278.

[23] *Study on channel model for frequencies from 0.5 to 100 GHz (Release 16)*, 3GPP TR 38.901, 2019.

[24] V. T. Ermolaev, "Evaluation of parameters for the minimal polynomial of the signal-correlation matrix of a multichannel adaptive receiving system," *Radiophysics and Quantum Electronics*, vol. 38, no. 8, pp. 551–561, 1995. DOI: 10.1007/bf01037705.